Output-Feedback Control of a Piezomicropositioning Tube Actuator with Uncertain Nonlinearities

Mohammad Al Janaideh, Almuatazbellah M. Boker, and Micky Rakotondrabe

***Abstract*— In [1] we proposed output-feedback tracking control with an extended high-gain observer-based feedback control for a class of systems that include unknown hysteresis nonlinearities. In this paper, we proposed the control system for a piezomicropositioning tube actuator with uncertain nonlinearities. The proposed control system has a number of features; namely, (i) it can guarantee ultimate boundedness of the tracking error, where the ultimate bound can be made arbitrarily small, for any given initial conditions and for bounded unknown exogenous inputs and modeling parameters, (ii) it provides the possibility of shaping the transient response of the closed-loop system as desired, and (iii) the proposed technique is non-adaptive inversion free technique. In this study, we developed the proposed output-feedback approach for precision motion system, and we applied this approach experimentally to a piezotube micro-positioning actuator. The main contribution of this paper is to show that an extended high-gain observer-based output-feedback control system can stabilize a class of precision motion systems with unknown hysteresis nonlinearties.**

I. INTRODUCTION

Considerable works have been led in the modeling and control of piezomicropositioning systems by accounting for their hysteresis nonlinearities in order to reach certain accuracy in the final tasks. Different control techniques have been proposed to stabilize these systems with hysteresis nonlinearities. These techniques can be classified into inversion-based and inversion free-based control systems. Inversion-based control systems consider the inverse hysteresis model as a feedforward compensator to reduce the effect of hysteresis nonlinearities. These include inverse Preisach model, inverse Prandtl-Ishlinskii model, inverse rate-dependent Prandtl-Ishlinskii model, inverse generalized Prandtl-Ishlinskii model. These inverse models have been used with different feedback control techniques to enhance the performance of the compensation. For instance, robust control [2], [3], PID control [3], sliding mode control [4], and extended high-gain observer based control [5] have been combined with inverse hysteresis. These techniques assume known hysteresis nonlinearties within the closed-loop control systems [5].

M. Al Janaideh is with the Department of Mechanical Engineering, Memorial University, St. John's, NL A1B 3X5, Canada. email: maljanaideh@mun.ca.

A. Boker is with the Bradley Department of Electrical and Computer Engineering, Virginia Tech, Blacksburg, VA 24060, USA. e-mail: boker@vt.edu.

M. Rakotondrabe is with the National School of Engineeringin Tarbes (ENIT - INPT), University of Toulouse, 65000 Tarbes France e-mail: mrakoton@enit.fr.

Other approaches fall under the inversion free-based control systems. These include disturbance rejection [6], adaptive control for Prandtl-Ishlinskii model [5], an inversion-free feedforward rate-dependent compensator for the rate-dependent Prandtl-Ishlinskii model [7], a multiplicative structure to compensate for the Bouc-Wen hysteresis nonlinearity in piezoelectric actuators [8], and retrospective cost adaptive control [9].

The contributions of this paper include the application of inversion-free adaptive-free control approach for a piezoelectric micropositioning system that deals with uncertain hysteresis dynamics and high oscillations. Based on the seminal work [10], [11], we utilize an extended high-gain observer-based control strategy to stabilize a wide class of precision motion systems. Following this strategy, we show experimentally that it is possible to robustly track any desired reference signal for any given initial conditions with the possibility to shape the transient performance of the closed-loop system.

The remainder of the paper is organized as follows. Section II introduces the problem formulation. In Section III, a closed-loop system with the unknown nonlinearities is considered. Then section VI presents experimental results of the proposed high-gain observer-based output feedback control with piezoelectric actuator classically employed in precise positioning applications such as in atomic force microscopy and in nanomanipulation. The piezoelectric actuator shows rate-dependent hysteresis, creep effects, and high oscillations. Finally, the conclusion and future work are presented in Section V.

II. PROBLEM FORMULATION

We consider precision motion system represented by the following nonlinear model

$$\begin{aligned} \dot{x}_1 &= x_2, \\ \dot{x}_2 &= a(x, w) + \psi(\eta) + \rho(t) + u, \end{aligned} \quad (1)$$

$$\epsilon\dot{\eta} = \Phi(x, \eta), \quad (2)$$

$$\dot{w} = f_0(x, w), \quad (3)$$

$$y = x_1, \quad (4)$$

where $x \in \mathbb{R}^2$, $w \in \mathbb{R}^q$, $u \in \mathbb{R}$ and $y \in \mathbb{R}$ are the state, control input and measured output, respectively, $\psi(\eta)$ is a function that represents the output of the hysteresis dynamics and $\eta \in \mathbb{R}^n$ is the state of the hysteresis dynamics. In this study we consider the Netushil hysteresis system, and more details can be found in [1][12], ϵ is a positive small constant, $\rho(t) \in \mathbb{R}$ is an unknown bounded disturbance, and $a(\cdot, \cdot)$

and $f_0(\cdot,\cdot)$ are assumed to be sufficiently smooth and locally Lipschitz nonlinear functions (could be unknown). The equations $\epsilon\dot{\eta} = \Phi(0, \eta)$, and $\dot{w} = f_0(0, w)$ constitute the zero dynamics of the system, i.e. the remaining dynamics of the system when $y = 0$ [13]. Accordingly, the internal dynamics are based on the zero dynamics. In [1], we show that (2) is bounded-input-bounded state stable. We further assume that (3) is bounded-input-bounded state stable making the whole internal dynamics bounded-input-bounded state stable. More specifically, we have the following assumption.

Assumption 2.1: There is a continuously differentiable function $V_0(w)$, class K functions ρ_1 and ρ_2, and a nonnegative continuous non-decreasing function χ such that

$$\rho_1(||w||) \leq V_0(w) \leq \rho_2(||w||)$$
$$\frac{\partial V_0}{\partial w} f_0(x, w) \leq 0, \quad \forall\ ||w|| \leq \chi(||x||)$$

for all $x, w \in \mathbb{R}^m \times \mathbb{R}^q$.

We consider the problem of controlling the output $y(t)$ so that it asymptotically tracks a reference signal $d_1(t)$. In this case, we assume that $d_1(t)$ is a smooth bounded function and $d_2 \triangleq \frac{dd_1}{dt}$ to be bounded for all $t \geq 0$. The closed-loop system's transient response is desired to have some predefined characteristics such as particular settling time and percentage overshoot. Towards accomplishing this objective, we consider the change of variables

$$e = x - d,$$

where $e = [e_1\ e_2]^T$, and $d = [d_1\ d_2]^T$. Using this change of variables, we get the tracking error dynamics

$$\dot{e}_1 = e_2, \tag{5}$$
$$\dot{e}_2 = a(e + d, w) + \psi(\eta) + \rho(t) + u - \dot{d}_2, \tag{6}$$
$$\epsilon\dot{\eta} = \Phi(e + d, \eta), \tag{7}$$
$$\dot{w} = f_0(e + d, w), \tag{8}$$
$$y_t = e_1 = x_1 - d_1, \tag{9}$$

where y_t is the measured tracking error. The problem can now be cast as designing a controller u to asymptotically regulate $e(t)$ to zero while meeting certain requirements on the transient response. In [1], a linear combination of weighted Netushil hysteresis operators can be presented as

$$\psi(\eta) = \sum_{i=0}^{n} p_i \eta_i, \tag{10}$$

where

$$\epsilon\dot{\eta}_i(t) = \Phi_{r_i}[z_i](t), \tag{11}$$
$$z_i(t) = v(t) - \eta_i(t) \tag{12}$$
$$\eta_i(0) = \eta_{i0}, \tag{13}$$

where $v \in \mathbb{R}$ is the input, $p_i \geq 0$ are positive constants, $i = 1, 2, \ldots, n$, $\eta_i(0)$ are initial conditions, $r_i \geq 0$ are thresholds that determine the radius of the hysteresis loops, and $\Phi_{r_i}[z_i](t)$ are the output of the deadzone operators. More details on the model can be found in [1]. We can write

$$|\psi| \leq np_{\max}|v| + np_{\max}|\sigma|, \tag{14}$$

where $\sigma = \eta_i - v$ is the shift of the operator due to the term $\epsilon\dot{\eta}_i$. Then, the bounds of the model depends on the input $v(t)$ and ϵ. We can show that the hysteresis model is bounded-input-bounded-state stable when viewing v as input. For this purpose, we consider the Lyapunov function $V_{1i}(\eta_i) = \frac{1}{2}\eta_i^2$. It can be shown that the derivative of $V_{1i}(\eta_i)$ takes the following piecewise linear form

$$\leq \begin{cases} -\frac{1}{2\epsilon}\eta_i^2, & \forall\ |\eta_i| \geq 2\epsilon(|v| - |r_i|), \\ & \text{if} \quad \eta_i < v - r_i\ \&\ \dot{v} > 0, \\ & \text{or if} \quad \eta_i > v + r_i\ \&\ \dot{v} < 0, \\ 0, & \text{if} \quad |v - \eta_i| < r_i. \end{cases} \tag{15}$$

The segment inequalities (15) with Assumption 2.1 imply the internal dynamics are bounded-input-bounded-state stable.

III. High-gain Observer-Based Control of Precision Motion Systems with Hysteresis

In this section we review the control design in [1] for a micropositioning system of a second order system with hysteresis and creep nonlinearities. The proposed control strategy is based on employing a feedback linearization control assuming first that the states as well as the hysteresis nonlinearity and exogenous inputs are known. This way, the transient performance can be shaped as desired by choosing the eigenvalues of the closed-loop system. Considering now the realistic scenario where only the measured output is available for feedback and that modeling of the system nonlinearities and exogenous inputs may not be precise, we utilize an extended high-gain observer to estimate the unavailable states and system nonlinearities. Using this approach, it can be seen that the standard features of high-gain observer-based control systems are attainable. In particular, the closed-loop system can track any bounded reference signal in a robust way and for any given initial conditions.

As a step towards solving the control problem, in what follows, we will design an extended high-gain observer to estimate the state vector e as well as the nonlinear and/or the unknown terms included in equation (6). We will then design a stabilizing controller that makes use of the estimated information. As will be shown later, the estimation of the unknown functions is possible since we will assume that these collectively constitute an extended state of the system. This helps in mitigating any errors associated with the modeling process of the hysteresis and the modeling of the exogenous input.

A. State-feedback Controller

Our choice of utilizing a high-gain observer implies that the estimates of e and $\kappa \triangleq a(e + d, w) + \psi(\eta) + \rho(t) - \dot{d}_m$ will be provided in a relatively fast time. As a result, we can design a controller as if this information is available for feedback [14], [15], [16]. This leads to the feedback linearization control

$$u = -\kappa - k_1 e_1 - k_2 e_2 \tag{16}$$

The closed-loop system is then given by

$$\dot{e} = A_c e, \tag{17}$$

$$\epsilon\dot{\eta}_i = \Phi_{r_i}[e + d - \eta_i](t), \quad i = 1, 2, \ldots, n, \tag{18}$$

$$\dot{w} = f_0(e + d, w), \tag{19}$$

where

$$A_c = \begin{bmatrix} 0 & 1 \\ -k_1 & -k_2 \end{bmatrix} \in \mathbb{R}^{2\times 2}$$

and k_1 and k_2 are positive constants chosen so that A_c has desired eigenvalues. Next, we design the observer to provide the missing information in (16).

B. High-gain Observer-based Output Feedback Control

Consider the system (5)-(6), then an extended high-gain observer can be given as

$$\dot{\hat{e}}_1 = \hat{e}_2 + \frac{\alpha_1}{\mu}(y_t - \hat{e}_1), \tag{20}$$

$$\dot{\hat{e}}_2 = \hat{\kappa} + u + \frac{\alpha_2}{\mu^2}(y_t - \hat{e}_1), \tag{21}$$

$$\dot{\hat{\kappa}} = \frac{\alpha_3}{\mu^3}(y_t - \hat{e}_1), \tag{22}$$

where $\mu > 0$ is a small parameter to be designed, y_t is given by (9) and $\alpha_1, \alpha_2, \alpha_3$ are chosen such that the polynomial $s^3 + \alpha_1 s^2 + \alpha_2 s + \alpha_3 = 0$ is Hurwitz. Combining (20)-(22) with (16) leads to the output-feedback control

$$u = M\text{sat}\left(\frac{-\hat{\kappa} - k_1 e_1 - k_2\hat{e}_2}{M}\right), \tag{23}$$

where $\text{sat}(\cdot)$ is the saturation function. The saturation is used to protect the system from peaking in the observer's transient response [17]. The saturation limits $\pm M$ are chosen to be outside of the compact set that is based on the initial condition, that is $M > \max_{\text{(set of initial conditions)}} |-\kappa - k_1 e_1 - k_2 e_2|$. Notice that the output-feedback controller (23) does not require the knowledge of the derivatives of d_1. The design procedure can now be summarized as follows: we first design the state-feedback controller that assigns the appropriate closed-loop eigenvalues that would result in the desired performance. Then, the extended high-gain observer-based output feedback controller is designed to recover the state-feedback performance. The recovery of performance happens as the observer parameter ϵ is selected to be sufficiently small. The caveat here is that a trade-off might be needed since pushing ϵ too small, or the observer gain to be too high, is likely to exacerbate the effect of noise. As it turned out, this issue was not a problem in our experimental procedure outlined in the next section.

IV. Application to a Piezomicropositioning Tube Actuator

The extended high-gain observer-based feedback is proposed in this section to control a piezomicropositioning tube actuator. This section includes experimental setup, system modeling, control design, and experimental results. This actuator shows rate-dependent hysteresis, creep effects, and oscillations.

A. The actuator and the experimental setup

The piezoelectric actuator, displayed in Figure (1-a) and called piezomicropositioning tube actuator, has a cylinder shape with internal hole. It has four external electrodes and one internal electrode for electrical ground. According to which of the four external electrodes are subjected to electrical potential (voltage), the piezomicropositioning tube actuator bends along the x-axis or along the y-axis. On the other hand, if all the four external electrodes receive the same electrical potential, the actuator expands along its axis (z-axis). A piezomicropositioning tube actuator can therefore perform x-y-z movement. piezomicropositioning tube actuators are classically used in precise positioning applications such as atomic force microscopes for images scanning [18] and positioners for micro- and nano-manipulation [19]. In fact piezomicropositioning tube actuator can provide high resolution (down to nanometers) and large bandwidth (up to hundreds of Hertz).

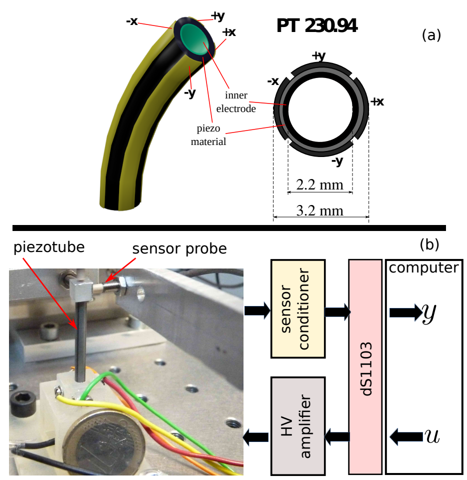

Fig. 1: (a) The piezomicropositioning tube actuator used in the experiment, and (b) the experimental setup.

In this section we test the proposed high-gain observer-based output feedback control in the direction of y-axis. The experimental setup is displayed in Figure (1-b) and is composed of: (i) the piezomicropositioning tube actuator: the actuator itself, referenced as PT 230.94 which has 30mm of length and 3.2 mm of external diameter. The internal hole of the piezomicropositioning tube has 2.2 mm of diameter. The piezotube can be driven with a voltage u up to ± 200 V but we limit in this paper the operating range to ± 150 V because of the limitation of the voltage amplifier. Meanwhile, the input range of ± 150V is sufficient to observe the hysteresis of the actuator and to analysis the controller performances proposed in this paper. (ii) Sensor: an inductive sensor with its probe is placed in front of the tip of the piezomicropositioning tube actuator to measure its y displacement. The sensor is the ECL202 and can provide 30 nm of resolution with a bandwidth of 15 kHz. Data acquisition: a computer with Matlab-Simulink in which the driving voltage u is generated, the measurement y is acquired and the controllers are implemented. A dSPACE acquisition board (dS1103) serves as converters between the numerical signals in the computer and the analogical signals from and to the piezotube actuator. (iv) Amplifier: a high-voltage (HV) amplifier that amplifies by 20 times the voltage from the computer-dSPACE board, limited to ± 10 V.

B. Actuator nonlinear dynamics

In order to obtain the piezomicropositioning tube actuator dynamics, first we apply a sinusoidal input (driving) voltage. An amplitude of 150 V has been used at different excitation frequencies between 0.1 Hz and 200 Hz. Figure 2 shows the obtained displacement versus the input voltage over different excitation frequencies. Beyond the hysteresis nonlinearity property and the fact that its shape changes versus the frequency (rate-dependency), it shows that the range of displacement is about ± 30 μm for a voltage of ± 150 V, i.e. the gain is $5[\frac{\mu m}{V}]$. Such a gain is high and thus interesting when comparing to other piezoelectric cantilevered actuators devoted to precise positioning tasks [20]. Then, we apply a step input voltage of 150 V to the piezomicropositioning tube actuator. The measured output displacement is depicted in Figure 3, which clearly shows the badly damped oscillations property. A quick identification shows that the first resonant frequency is of 776Hz and the settling time is approximately 19 ms. Moreover, the response shows a low-rate drift (can be seen at 0.1 Hz in Figure 2). This drift is called creep phenomenon and is typical for piezoelectric actuators. Similar to hysteresis, the creep phenomenon introduces precision loss in the tasks to be carried out and should therefore be controlled.

In this section we consider the following system to model the nonlinear dynamics of the piezomicropositioning tube actuator

$$\dot{x}_1 = x_2 \tag{24}$$

$$\dot{x}_2 = -a_2 x_2 - a_1 x_1 + \mathcal{P}(u,\eta) + \xi, \tag{25}$$

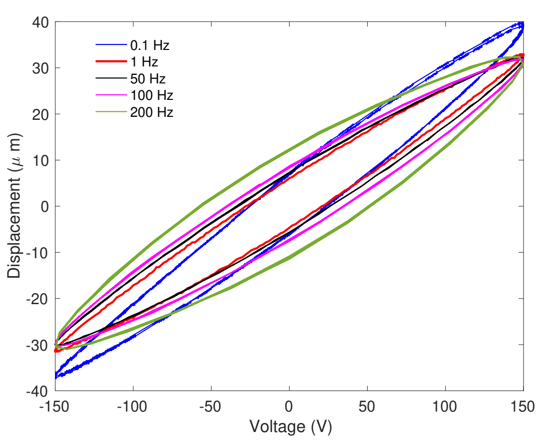

Fig. 2: Measured hysteresis loops of the piezomicropositioning tube actuator under a sinusoidal voltage with $150V$ of amplitude at 0.1 Hz, 1 Hz, 50 Hz, 100 Hz, and 200 Hz.

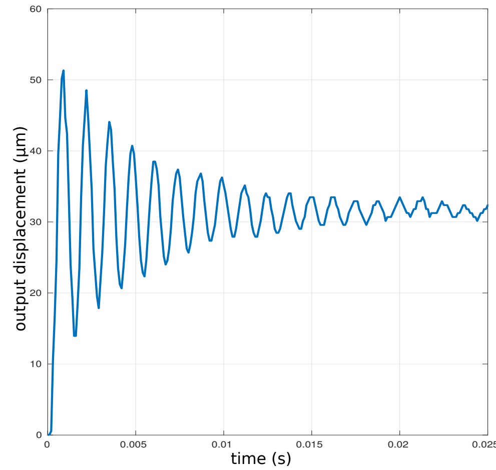

Fig. 3: Step response of piezomicropositioning tube actuator with $150V$ of input voltage.

where $\xi(t)$ represents bounded unknown disturbances and unmodelled dynamics, $\mathcal{P}(u,\eta) = p_0 u + \sum_{i=1}^{n} p_i \eta_i$, $\epsilon \dot{\eta}_i = \Phi_{r_i}[u - \eta_i]$, and $y(t) = x_1(t)$. It is important to mention that we consider uncertain hysteresis and creep nonlinearities with second order system to present the oscillations of the piezomicropositioning tube actuator. The parameters of the model are $a_1 = 23903519, a_2 = 293$, and $p_0 = 2511930$. More details about the system (24)-(25) can be found in [2] and [21].

C. Output-feedback Controller

Following the procedure outlined in Section III-B, an extended high-gain observer can be designed in the form of

$$\dot{\hat{e}}_1 = \hat{e}_2 + \frac{\alpha_1}{\mu}(y_t - \hat{e}_1) \tag{26}$$

$$\dot{\hat{e}}_2 = -a_1 \hat{e}_1 - a_2 \hat{e}_2 + \hat{\kappa} + p_0 u + \frac{\alpha_2}{\mu^2}(y_t - \hat{e}_1) \tag{27}$$

$$\dot{\hat{\kappa}} = \frac{\alpha_3}{\mu^3}(y_t - \hat{e}_1), \tag{28}$$

where $y_t = e_1 = y - d_1$ and d_1 is the desired input. The observer parameters are chosen to be $\alpha_1 = 6, \alpha_2 = 11, \alpha_3 = 6$, and $\mu = 0.00001$. It is important to note here that $\hat{\kappa}$ now provides an estimate of $\sum_{i=1}^{n} p_i \eta_i - a_1 d_1 - a_2 d_2 - d_3$, where d_2 and d_3 are the first and second derivatives of d_1, respectively. The estimates from (26)-(28) will then be used in

$$u = \frac{M}{p_0} \mathrm{sat}\left(\frac{-\hat{\kappa} - k_1 e_1 - k_2 \hat{e}_2}{M} \right). \tag{29}$$

The saturation level is chosen to be $M = \pm 500$ to be sure that it will not saturate the experimental driving voltage and thus create unwanted oscillations. The controller gains are chosen as $k_1 = 900000000, k_2 = 0$. Notice that because the linear parts of the system in equation (25) are known and providing damping (stabilizing) effect, the controller is designed to not cancel them. This lead to the choice that $k_2 = 0$. It should also be noted that these gains were chosen as initial setting, however they can be tuned afterwards for better performances of the closed-loop if required. The output-feedback controller is afterwards applied to the experimental piezomicropositioning tube actuator.

First a series of step input as reference y_{ref} is applied to the closed-loop which includes the piezomicropositioning tube actuator. Figure 4 presents the results where the output y is compared with the desired displacement y_{ref}. As we can observe, the output tracks the input reference and no creep (drift) appears in the output displacement and the oscillations are damped. Then, a varying input desired displacement is applied to verify tracking performance with a different desired input displacement. Figure 5-a displays the results when the desired displacement varies between $-30\mu m$ to $30\mu m$. Figure 5-b shows the tracking error and the which the root-mean-square of the tracking error is $0.326\mu m$.

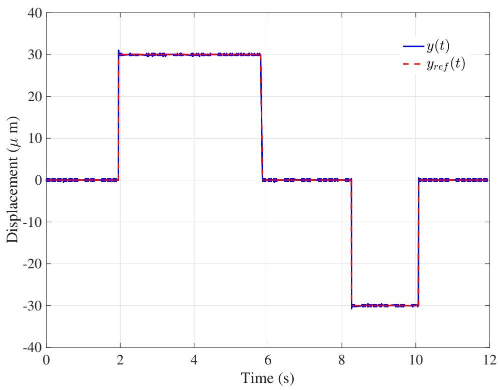

Fig. 4: Comparison between the desired step displacement and output displacement with proposed control.

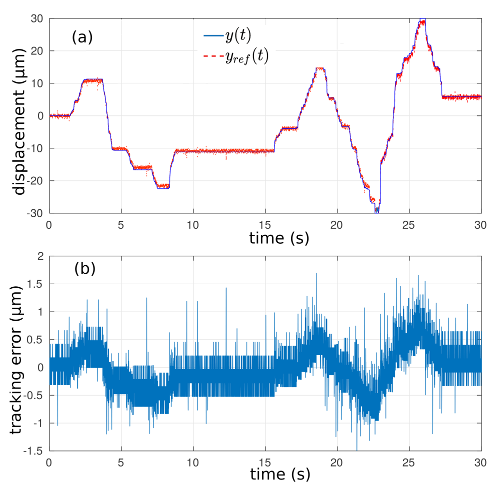

Fig. 5: Tracking performance of the proposed control system with a varying signal: (a) comparison between the desired and output displacement with the proposed control (29), (b) tracking error of (a).

Then the time domain performances of the closed-loop with the proposed controller is analyzed through a step response (desired displacement). Figure 6 shows the measured step response and the simulated step response when a desired displacement of $30\mu m$ is applied. In order to compare the performances of the proposed controller with those in the literature, we considered the feedforward-feedback controller of the same piezotube actuator that is recently proposed in [22]. In [22], the hysteresis is compensated with the inverse rate-dependent Prandtl-Ishlinskii hysteresis compensator and a Reference Signal Tracking structured designed with interval techniques. As depicted in Figure 6, the proposed closed-loop technique has better response time than the closed-loop control in [22]. The proposed controller exploits the internal dynamics of the actuator (state estimation) and this allows to perform better dynamics in the closed-loop systems.

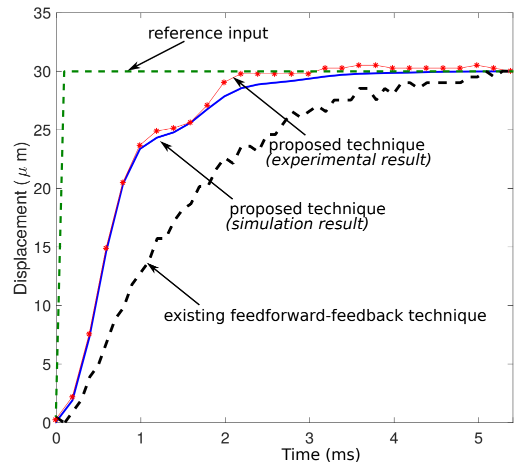

Fig. 6: Comparison between step desired displacement and output displacement with the proposed inversion-free control signal (29) and inversion-based control technique in [22].

Then a harmonic analysis is performed. A sinusoidal shaped desired displacement y_{ref} with an amplitude of $30\mu m$ and an excitation frequency between $\approx 1.5Hz$ ($10\frac{rad}{s}$) and $1.7KHz$ ($10681\frac{rad}{s}$) is used. Figure 7 illustrates the resulting magnitude, the magnitude of the open-loop, and the magnitude of the closed-loop with the feedforward-feedback controller in [22]. The results show that the resonance at $776Hz$ ($4880\frac{rad}{s}$) is damped by the two closed-loop control systems (the proposed extended high-gain observer-based control and the feedforward-feedback controller). However, the proposed extended high-gain observer-based control approach shows a higher bandwidth.

Table (I) summarizes the performances of the proposed controller in Figure 6 with closed-loop control system in [22]. The results clearly indicate that the proposed controller propose the best combination of the performances in comparison with the controller proposed in [22].

V. Conclusions

We show that, for piezomicropositioning systems with uncertain hysteresis, it is possible to follow an extended high-gain observer-based approach to solve the output feedback tracking problem. In this way, one can first design a feedback linearzing control, assuming that all the states and the model

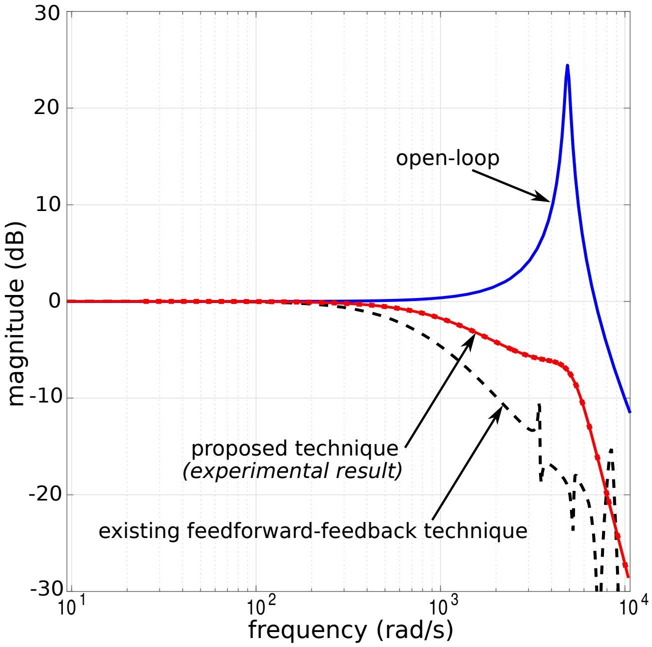

Fig. 7: The frequency responses of the piezomicropositioning tube actuator with and without control system and with inversion-based control technique in [22].

TABLE I: Performances summary of open-loop, proposed closed-loop inversion-free control system, and closed-loop inversion-based control system (the feedforward-feedback controller) [22].

	Open loop	Proposed controller (simulation)	Proposed controller (experimental)	Controller of [22]
Settling time	$\approx 19ms$	$\approx 2.2ms$	$\approx 1.8ms$	$\approx 4ms$
Static error		0%	0%	0%
Overshoot	$\approx 57\%$	0%	0%	0%
Bandwidth	1209Hz (7600$\frac{rad}{s}$)	—	265Hz (1660$\frac{rad}{s}$)	117Hz (737$\frac{rad}{s}$)

information are available, to shape the transient response of the closed-loop system. An extended high-gain observer can then be utilized to provide the missing information in a relatively fast time. As a result, it is possible for the output feedback controller to robustly recover the performance of the state feedback controller. It is important to mention that the proposed feedback controller of this study assumes uncertain hysteresis nonlinearities and partially known dynamics.

Acknowledgement

This work was supported by the Natural Sciences and Engineering Research Council of Canada and the Embassy of France in Ottawa.

References

[1] M. Al Janaideh and A. Boker, "Modeling and output-feedback control of systems with netushil rate-dependent hysteresis nonlinearties," in *Proceedings of the IEEE Conference on Decision and Control*, Miami Beach, FL, pp. 6912–6917, 2018.

[2] M. Al Janaideh, M. Rakotondrabe, and O. Aljanaideh, "Further results on hysteresis compensation of smart micropositioning systems with the inverse prandtl-ishlinskii compensator," *IEEE Transactions on Control Systems Technology*, vol. 24, pp. 428–439, 2016.

[3] L. Riccardi, D. Naso, B. Turchiano, and H. Janocha, "Design of linear feedback controllers for dynamic systems with hysteresis," *IEEE Transactions on Control Systems Technology*, vol. 22, pp. 1268–1280, 2014.

[4] M. Edardar, X. Tan, and H. Khalil, "Design and analysis of sliding mode controller under approximate hysteresis compensation," in *IEEE Transactions on Control Systems Technology*, vol. 23, 2014, pp. 598–608.

[5] D. Chowdhury, Y. K. Al-Nadawi, and X. Tan, "Hysteresis compensation using extended high-gain observer and dynamic inversion," in *Proceedings of the ASME Dynamic Systems and Control Conference*, Atlanta, GA, pp. 1–9, 2018.

[6] M. Al Janaideh and A. El-Shaer, "Performance enhancement for a class of hysteresis nonlinearities using disturbance observers," *International Journal of Control, Automation and Systems*, vol. 12, pp. 283–293, 2014.

[7] M. Al Janaideh, M. Rakotondrabe, I. Darabsah, and O. Aljanaideh, "Internal model-based feedback control design for inversion-free feedforward rate-dependent hysteresis compensation of piezoelectric cantilever actuator," *Control Engineering Practice*, vol. 72, pp. 29–41, 2016.

[8] M. Rakotondrabe, "Bouc-wen modeling and inverse multiplicative structure to compensate hysteresis nonlinearity in piezoelectric actuators," *IEEE Transactions on Automation Science and Engineering*, vol. 8, pp. 428–431, 2011.

[9] M. Al Janaideh and D. S. Bernstein, "Adaptive control of uncertain hammerstein systems with hysteretic nonlinearities," in *Proceedings of the IEEE Conference on Decision and Control*, Los Angeles, CA, pp. 545–550, 2014.

[10] L. Freidovich and H. Khalil, "Performance recovery of feedback-linearization-based designs," *IEEE Transactions on Automatic Control*, vol. 53, pp. 2324–2334, 2008.

[11] H. K. Khalil, "Extended high-gain observers as disturbance estimators," *SICE Journal of Control, Measurement, and System Integration*, vol. 10, pp. 125–134, 2017.

[12] C. Kuehn and C. Munch, "Generalized play hysteresis operators in limits of fast-slow systems," *SIAM Journal on Applied Dynamical Systems*, vol. 16, pp. 1650–1685, 2017.

[13] H. K. Khalil, *Noninear systems*. Prentice-Hall, New Jersey, 1996.

[14] A. M. Boker and H. K. Khalil, "Control of flexible joint manipulators using only motor position feedback: A separation principle approach," in *Proceedings of the IEEE Conference on Decision and Control*, Firenze, Italy, pp. 244–249, 2013.

[15] ——, "Semi-global output feedback stabilization of non-minimum phase nonlinear systems," *IEEE Transactions on Automatic Control*, vol. 62, pp. 4005–4010, 2016.

[16] ——, "Nonlinear observers comprising high-gain observers and extended kalman filters," *Automatica*, vol. 49, pp. 3583–3590, 2013.

[17] F. Esfandiari and H. Khalil, "Output feedback stabilization of fully linearizable systems," *International Journal of control*, vol. 56, pp. 1007–1037, 1992.

[18] G. Binnig and D. Smith, "Single-tube three-dimensional scanner for scanning tunneling microscopy," *Review of Scientific Instruments*, vol. 57, pp. 1688–1689, 1986.

[19] H. Xie, M. Rakotondrabe, and S. Regnier, "Characterizing piezoscanner hysteresis and creep using optical levers and a reference nanopositioning stage," *Review of Scientific Instruments*, vol. 80, pp. 1–3, 2009.

[20] M. Rakotondrabe, *Smart materials-based actuators at the micro/nano-scale: characterization, control and applications*. Springer, New York, ISBN 978-1-4614-6683-3, 2013.

[21] M. Al Janaideh, M. Rakotondrabe, I. Darabsah, and O. Aljanaideh, "Internal model-based feedback control design for inversion-free feedforward rate-dependent hysteresis compensation of piezoelectric cantilever actuator," *Control Engineering Practice*, vol. 72, pp. 29–41, 2016.

[22] M. Rakotondrabe and M. Al Janaideh, "An RST control design based on interval technique for piezomicropositoning systems with rate-dependent hysteresis nonlinearities," in *Proceedings of the IEEE Conference on Decision and Control*, Nice, France, pp. 6833–6838, 2019.